HHS Public Access

Author manuscript

Cell Rep. Author manuscript; available in PMC 2017 December 27.

Published in final edited form as:

Cell Rep. 2017 July 05; 20(1): 30–39. doi:10.1016/j.celrep.2017.06.022.

The Ubiquitination of PINK1 Is Restricted to Its Mature 52-kDa Form

Yuhui Liu[1,3,7], **Cristina Guardia-Laguarta**[1,3,7], **Jiang Yin**[4], **Hediye Erdjument-Bromage**[5], **Brittany Martin**[1,3], **Michael James**[4], **Xuejun Jiang**[6], and **Serge Przedborski**[1,2,3,8,*]

[1]Departments of Pathology and Cell Biology, Columbia University, New York, NY 10032, USA

[2]Department of Neurology, Columbia University, New York, NY 10032, USA

[3]Center for Motor Neuron Biology and Diseases, Columbia University, New York, NY 10032, USA

[4]Department of Biochemistry, University of Alberta, Edmonton, AB T6G 2H7, Canada

[5]Department of Biochemistry and Molecular Pharmacology, New York University, New York, NY 10016, USA

[6]Program in Cell Biology, Memorial Sloan Kettering Cancer Center, New York, NY 10065, USA

SUMMARY

Along with Parkin, PINK1 plays a critical role in maintaining mitochondrial quality control. Although PINK1 is expressed constitutively, its level is kept low in healthy mitochondria by polyubiquitination and ensuing proteasomal degradation of its mature, 52 kDa, form. We show here that the target of PINK1 polyubiquitination is the mature form and is mediated by ubiquitination of a conserved lysine at position 137. Notably, the full-length protein also contains Lys-137 but is not ubiquitinated. On the basis of our data, we propose that cleavage of full-length PINK1 at Phe-104 disrupts the major hydrophobic membrane-spanning domain in the protein, inducing a conformation change in the resultant mature form that exposes Lys-137 to the cytosol for subsequent modification by the ubiquitination machinery. Thus, the balance between the full-length and mature PINK1 allows its levels to be regulated via ubiquitination of the mature form and ensures that PINK1 functions as a mitochondrial quality control factor.

In Brief

PINK1 mutations cause Parkinson's disease. PINK1 is cleaved into a shorter 52-kDa form at the mitochondrial membrane, but regulation of the turnover of cleaved PINK1 is unknown. Liu et al. show that polyubiquitination of cleaved PINK1 regulates its degradation via the proteasome.

Correspondence: sp30@columbia.edu.

[7]These authors contributed equally

[8]Lead Contact

AUTHOR CONTRIBUTIONS

Y.L., X.J., and S.P. designed the research; Y.L., C.G.-L., J.Y., H.E.-B., and B.M. performed experiments; Y.L., J.Y., C.G.-L., M.J., H.E.-B., and S.P. analyzed the data; and Y.L., J.Y., and S.P. wrote the paper.

SUPPLEMENTAL INFORMATION

Supplemental Information includes Supplemental Experimental Procedures and four figures and can be found with this article online at http://dx.doi.org/10.1016/j.celrep.2017.06.022.

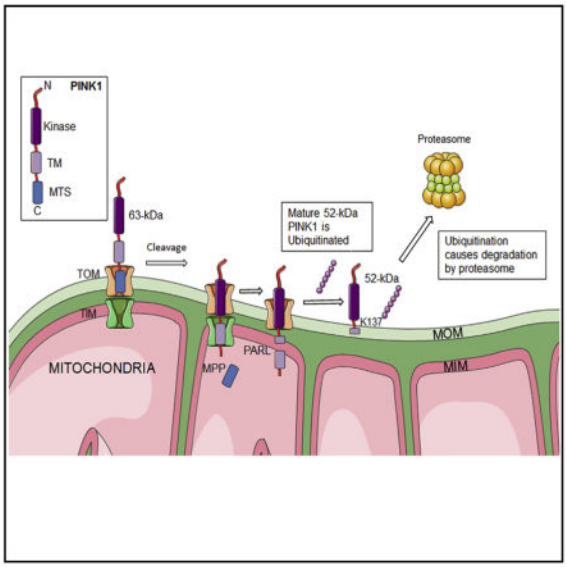

INTRODUCTION

Parkinson's disease (PD) is an adult-onset neurodegenerative disorder that is characterized histologically by the loss of ventral midbrain dopaminergic neurons and by the presence of intra-cytoplasmic proteinaceous inclusions, or Lewy bodies, in the few neurons that are spared (Dauer and Przedborski, 2003). In a subset of PD cases, mutations in *PINK1*, which encodes for a mitochondrial kinase, have been associated with an early-onset form of the disease, inherited as an autosomal recessive trait (Valente et al., 2004).

In energized mitochondria, full-length PINK1 (63 kDa) is rapidly imported and processed in two steps: first by the mitochondrial processing peptidase (MPP) to a 60-kDa intermediate form (cleavage between aa 34 and 35 [Greene et al., 2012; Jin et al., 2010]), and then by the presenilin-associated rhomboid-like protein (PARL) to a 52-kDa mature form (cleavage between aa 103 and 104 [Greene et al., 2012; Jin et al., 2010; Whitworth et al., 2008]). The 52-kDa form is located on the mitochondrial outer membrane (MOM) and retains most of the known functional properties of the full-length form (Sim et al., 2012).

Whereas the transcription of *PINK1* is high (Blackinton et al., 2007; Taymans et al., 2006; Unoki and Nakamura, 2001; Zhou et al., 2008), the steady-state levels of all three PINK1 protein species are unexpectedly low (Zhou et al., 2008). Although low mRNA stability might account for this finding, a second possibility is that some of the PINK1 polypeptide species, and especially the fully processed mature 52-kDa form, are turned over rapidly. In support of this second possibility, it has been found that PINK1 is ubiquitinated, but which of the three PINK1 species is modified is not known (Shiba et al., 2009; Zhou et al., 2008).

We show here that mature, but not full-length, PINK1 is polyubiquitinated and that its level is kept low in healthy mammalian mitochondria via a specific ubiquitination at Lys-137 (K137), followed by subsequent proteasomal degradation.

RESULTS

Ubiquitinated PINK1 Is Anchored Primarily to Mitochondria

The ubiquitin/proteasome system is known to degrade MOM proteins, such as mitofusins (Tanaka et al., 2010), in damaged mitochondria. To test whether the same process applies to PINK1, we first asked whether ubiquitin is attached covalently to PINK1. We thus transfected influenza hemagglutinin (HA)-tagged ubiquitin (HA-Ub) into a stable human HEK293T cell line, in which exogenous PINK1 expression is ~3–5 times less than that in transiently transfected cells in the presence or absence of the proteasome inhibitor MG132. As described previously (Vives-Bauza et al., 2010), lysates from transfected cells with normal mitochondrial membrane potential were immunoprecipitated with anti-PINK1 and western blotted to reveal the HA tag. A HA-immunopositive smear was detected, most prominently after treatment with MG132 (Figure 1A, upper panel). When these blots were re-probed with anti-PINK1, an immunopositive smear was observed (Figure 1A, lower panel), implying that PINK1 is ubiquitinated covalently. In addition, these polyubiquitinated PINK1 (Ub-PINK1) bands were resistant to treatment with Empigen BB, a denaturing detergent to weaken protein-protein interaction without disrupting the high-affinity antigen-antibody interactions (Figure S1A), supporting that polyubiquitinated bands were generated directly from PINK1. Ub-PINK1 was also observed in other cell lines treated similarly (Figures S1B and S1C). We also detected Ub-PINK1 in cells harboring endogenous PINK1, ubiquitin, or both (Figures S1D–S1G), implying that the endogenous ubiquitination machinery can modify endogenous PINK1. Of note, among different clonal cell lines that we screened, we only consistently detect endogenous Ub-PINK1 species (Figure S1G) in a BE(2)-M17 neuroblastoma cell line that stably expresses human wild-type α-synuclein (Guardia-Laguarta et al., 2014). Finally, upon exposure of cells to 1 μM valinomycin to collapse $\Delta\Psi m$, Ub-PINK1 was reduced dramatically in experimental conditions described above (Figures 2F and S1H). These results indicate that Ub-PINK1 is a prominent feature of healthy mammalian mitochondria.

To determine the subcellular location of Ub-PINK1, we prepared crude cytosolic and mitochondrial fractions from HEK293T cells co-transfected with HA-Ub and PINK1. Ub-PINK1 species were strongly detected in the crude mitochondrial, but not cytosolic, fractions (Figure 1B). When these crude mitochondrial preparations were exposed to varying concentrations of proteinase K, the immunoreactivity for Ub-PINK1 declined in parallel with that of the MOM protein TOM70, whereas the intermembrane space (IMS) protein SMAC was unaffected (Figure 1C). Furthermore, when crude mitochondrial preparations were incubated with an alkaline extraction buffer, Ub-PINK1 was recovered primarily in the particulate fraction (Figure 1D). These results indicate that Ub-PINK1 is anchored in the MOM, presumably facing the cytosol.

The 52-kDa Mature PINK1 Fragment Is the Predominant Ubiquitinated Species

The above data showed that PINK1 is ubiquitinated, but did not reveal which PINK1 species is modified. There are 21 lysine residues in PINK1, with one (K24) located in the mitochondrial-targeting sequence (MTS), three (K114, K135, and K137) in the region connecting the main putative transmembrane domain and the kinase domain, 11 within the

kinase domain, and six in the region downstream of the kinase domain (Figure 2A). Except for K24, all of the lysine residues are present in both the 63-kDa and 52-kDa species. However, we and others (Jin et al., 2010; Lin and Kang, 2008; Takatori et al., 2008; Zhou et al., 2008) have found that proteasome inhibition increases the cellular content of 52-kDa PINK1 markedly more than that of 63-kDa PINK1. This finding suggests that the two main species may not interact with the ubiquitin-proteasome system equally, despite sharing the same set of internal lysine residues.

Thus, we set out to determine whether there was a difference in the ubiquitination pattern between the two main PINK1 species. The molecular mass difference between 63-kDa and 52-kDa PINK1 (i.e., 11 kDa) is approximately the same as of ubiquitin (~8.5 kDa), making it challenging to determine whether cleaved PINK1, full-length PINK1, or both is ubiquitinated. To circumvent this problem, we performed an in vivo ubiquitination assay using two different antibodies to PINK1: one raised against residues G51-R68 in the N terminus (denoted “N-term”) that only recognizes the 63-kDa PINK1 (see Figure 2B), and the other raised against residues M175-A250 (denoted “PINK1”) that recognizes both 63-kDa and 52-kDa forms (Figure 2B). Ub-PINK1 was detected by anti-HA following immunoprecipitation (IP) of cell lysates with the PINK1 antibody, but was barely detectable following IP with the N-term antibody (left panels in Figure 2D). Similar results were obtained for the reciprocal experiment, i.e., IP with anti-HA and blotting with either the PINK1 or N-term antibody (right panel in Figure 2D). To exclude the possibility that the apparent difference in the 63-kDa versus 52-kDa PINK1 ubiquitination was due to the differential affinity of the two anti-PINK1 antibodies, we generated a construct containing an internal Myc-tag, inserted between residues P34 and G35 of PINK1 (Myc^{34}-PINK1) (Figures 2C and S2A). Of note, the localization, cleavage, ubiquitin modification pattern, and induction of Parkin mitochondrial recruitment of Myc^{34}-PINK1 were comparable to that of the untagged PINK1 (Figures S2B, S2C, and S4A). A similar in vivo ubiquitination assay was then performed in HEK293T cells transiently co-transfected with Myc^{34}-PINK1 and HA-Ub. A robust Ub-PINK1 signal was revealed by the anti-HA antibody (much more intense in the presence of MG132) when the IP was performed with the anti-aa 175–250 PINK1 antibody. Conversely, it was faint when the IP was performed with the anti-Myc antibody (Figure 2E). These results imply that the Myc epitope inserted at aa 34–35 had been cleaved away from Ub-PINK1 due to PARL processing at aa 103–104 to generate the 52-kDa form.

Lastly, we performed an in vivo ubiquitination assay in cells, in which PINK1 cleavage was inhibited either chemically with 1 μM valinomycin or genetically by deletion of PARL, both of which prevent the conversion of the 63-kDa form to the 52-kDa form. Both strategies led to a decrease in the ratio of the 52-kDa:63-kDa forms, as expected (Jin et al., 2010; Narendra et al., 2010; Vives-Bauza et al., 2010), but surprisingly, there was also a striking reduction of Ub-PINK1 (Figures 2F and 2G). Taken together, our results provide strong evidence that 52-kDa, and not 63-kDa, PINK1 is the main target of ubiquitination.

If both the full-length and mature forms of PINK1 contain the same lysine residues (except for K24 in the MTS [see Figure 2A]), why is the full-length form “resistant” to ubiquitination? One possibility is that conformational changes triggered by the proteolytic

processing of full-length (un-ubiquitinated) PINK1 alter the presentation of the lysine residues that are the main targets for ubiquitination. To explore this possibility further, we used both homology-based modeling and de novo structure-prediction algorithms to determine the most likely conformations of PINK1 before and after proteolytic cleavage, applying criteria such as the structural conformity to experimentally determined kinase domains and the overall quality of the relationship of the geometry to that of reference models. The top-ranked inferred 3D models of 52-kDa PINK1 showed a well-folded kinase domain (between aa I218 and H515) that aligned with a root-mean-square deviation of 2.5 Å between the top models and a structural template (a calcium-dependent kinase; PDB: 3DXN). On the other hand, the region between F104 to I233 that constitutes the N terminus of 52-kDa PINK1 adopts a different conformation in some of the top predicted models, hinting that a greater degree of structural flexibility may exist in this part of the protein. A notable feature that was common to all of the top predicted models is that K114, K135, and K137 (the only lysine residues located in the linker region [see Figure 2A]) are all predicted to be surface residues exposed to the ambient environment (Figure 3A). Thus, we hypothesize that the cleavage of full-length PINK1 after A103 allows the linker region between the MTS and the kinase domain (aa F104–I233) to adopt a conformation, in which the internal lysine residues become more exposed to the aqueous phase (i.e., the cytosol).

Cytosol-Facing K137 Is a Major Ubiquitination Site of Mitochondrial PINK1

In light of the modeling predictions, we asked whether the above three lysine residues could be the main internal sites of ubiquitination in 52-kDa PINK1. We found that mutation of the only lysine residue in the MTS (K24R) or deletion of the first 111 amino acids (Δ1–111) had a marginal effect on Ub-PINK1 immunoreactivity, whereas deletion of the first 155 amino acids (Δ1–155) dramatically reduced it (Figures S2A and S2D). Thus, the main sites of PINK1 ubiquitination likely reside between amino acids 111 and 155, the region that includes only three lysines, namely, K114, K135, and K137. Next, we used mass spectroscopy to gain further insights into PINK1 internal ubiquitination sites. We co-transfected HEK293T cells with wild-type PINK1 and HA-Ub and treated the cells with MG132. Protein extracts were then immunoprecipitated with anti-PINK1, and the bands on the SDS-PAGE corresponding to ≥60 kDa (i.e., ≥52 kDa PINK1 + 1 Ub) were excised (Figure 3B), digested in-gel with trypsin, and analyzed by high-performance liquid chromatography with tandem mass spectrometry (LC-MS/MS) (Figure 3C). The analyses from three independent preparations resulted in 65% overall coverage of the PINK1 sequence (378/581 aa). Three unique lysine residues containing the -Gly-Gly modification indicative of covalent ubiquitin conjugation were identified in the excised gel: K137 (Figure 3C), K186, and K266 (Figure S3A); a fourth lysine, at K520, also gave a -Gly-Gly signature, but with a much lower degree of confidence (not shown). More-over, the Ub-PINK1 signal was not altered by the substitutions K186R or K266R (Figure S3B), suggesting that these two residues are unlikely to be predominant ubiquitination sites of PINK1. On the other hand, cells expressing the substitution K137R showed a profound reduction in the Ub-PINK1 signal as compared to wild-type PINK1 (Figure 3E). Furthermore, we found that the K137R mutation greatly stabilized PINK1 because it increased its half-life by ~20-fold (Figure 3F), with no evidence of PINK1 aggregation (Figures 4B, 4D, and 4E) (see below). Worth noting, accumulation of the 63-kDa K137R was also observed (Figures 3F and S4B).

Finally, by comparing the sequence alignment of PINK1 orthologs in different species (Figure 3D), we found that K137 is the most conserved of the three ubiquitin-modified residues identified in the spectroscopy analysis. We were unable to determine the ubiquitin modification of the lysine residues downstream of aa 363 due to the incomplete peptide coverage; hence, we cannot rule out the possibility that one of the uncovered lysine residues may also be ubiquitinated and contribute to PINK1 stability. Despite this caveat, our results support the importance of K137 in PINK1 ubiquitination and subsequent proteasome degradation.

The Polyubiquitin Chain on PINK1 Is Heterogeneous

Proteasomal degradation of polyubiquitinated proteins typically involves covalent ligation of the lysine residue on the target protein to K48 of ubiquitin. To determine if this was the case for PINK1, we mutated the seven lysine residues in ubiquitin (K6, K11, K27, K29, K33, K48, and K63) to arginine individually. Of the seven mutations, three—K29R, K48R, and K63R—yielded the strongest reductions in polyubiquitination. Interestingly, the K29R signal was associated with the most dramatic reduction in Ub-PINK1 signal, followed by K48R and K63R (Figure 3G), although by mass spectrometry, we were only able to detect the Ub-K48 -Gly-Gly signature (Figure S3C). These results suggest that PINK1 polyubiquitination consists of heterotypic chains, in which short initial K29-linked chains form longer mixed or branched chains composed primarily of K48 linkages and, to a much lesser extent, K63 linkages (Kravtsova-Ivantsiv et al., 2013; Kristariyanto et al., 2015; Michel et al., 2015).

Is 52-kDa PINK1 Degraded via the N-End Rule Pathway?

The above data imply that PINK1 degradation requires proteolytic cleavage of the full-length protein between A103 and F104 (Deas et al., 2011; Greene et al., 2012; Zhou et al., 2008), followed by ubiquitination at K137 to initiate subsequent proteasomal degradation. The mechanism by which this degradation occurs has been proposed to be via the N-end rule (Yamano and Youle, 2013) because the N terminus of 52-kDa PINK1 is phenylalanine, an N-end rule residue (Varshavsky, 2011). This mechanism implies that the N-terminal F104 protrudes from the MOM, facing the cytoplasm, where the three E3-ubiquitin ligases (UBR1, UBR2, and UBR4) that are required for protein degradation by the N-end rule pathway reside (Sriram and Kwon, 2010), but this topology was never confirmed (Yamano and Youle, 2013).

We therefore sought to define the sub-mitochondrial location of F104. We transfected cells with a construct, in which Myc was placed immediately before F104 (Myc^{104}-PINK1). As with Myc^{34}-PINK1 (described above), this mutant showed expression, cleavage, an ubiquitin modification pattern and induction of Parkin mitochondrial recruitment comparable to that of the untagged PINK1 (Figures S2B, S2C, and S4A). When the cells were treated with 0.01% digitonin to permeabilize the plasma membrane but not the MOM, no anti-Myc immunofluorescence signal was observed (Figure 4A), implying that F104 resides *inside* the mitochondria, where it presumably would not be accessible to cytosolic N-recognins (Sriram and Kwon, 2010), contrary to the predicted topology (Yamano and Youle, 2013). Of note, immunofluorescence to detect a Myc^{109}-PINK1 construct was positive

(Figure 4A), implying not only that the anti-Myc antibody was functional in the context of PINK1, but also that residues C-terminal to aa 109 face the cytoplasm (Zhou et al., 2008).

To help resolve the discrepancy between our and the published (Yamano and Youle, 2013) topologies for F104 predicted by the N-end rule, we asked if mutation of F104 to stabilizing (i.e., non-N-end rule) N-terminal residues, such as methionine or alanine (Varshavsky, 2011), increased PINK1 stability as described (Yamano and Youle, 2013). We found that these two substitutions indeed increased the half-life of 52-kDa PINK1 (from ~2.3 hr to ~6.4 hr [$PINK1^{F104A}$] and ~11.4 hr [$PINK1^{F104M}$]), consistent with the N-end rule (Sriram and Kwon, 2010) (Figure S4B). In addition, we assessed the PINK1 turnover rate in mouse embryonic fibroblasts (MEFs) deficient in the N-recognins required for degradation (Sriram and Kwon, 2010), as described (Varshavsky, 2011). As before, the lack of these three N-recognins was associated with an increased half-life of 52-kDa PINK1 (Figure S4C), again consistent with the N-end rule (Sriram and Kwon, 2010).

We were thus faced with the paradox of F104 residing inside mitochondria and yet apparently susceptible to degradation by the cytosolic N-end rule machinery. Because the N-end rule pathway requires that the N-recognins bind to the N-terminal residue, followed by ubiquitination at an internal target lysine, one would expect that if the N-end rule were operating on PINK1, Ub-PINK1 would be abolished in the $F104^{M/A}$ mutants. In fact, we found the opposite because neither mutation of F104 (Figure S4D) nor the deficiency of the N-recognins (Figure S4E) reduced PINK1 ubiquitination. Importantly, this unexpected discrepancy between PINK1 stability and ubiquitination was likely not an artifact because N-recognin-deficient MEFs transiently transfected with a known N-end rule substrate (Sindbis nonstructural proteins 4 [nsP4]) showed both increased half-life (Figure S4F) and decreased ubiquitination (Figure S4G), as expected.

If the N-end rule is not operating on PINK1, why are the $F104^{M/A}$ mutants long-lived? One possibility is that these PINK1 mutants were simply refractory to degradation. Consistent with this possibility, we found that upon transient transfection in HeLa cells, mutant $PINK1^{F104M/A}$ was prone to aggregation, as revealed by the presence of fluorescent PINK1 puncta, increased 52-kDa PINK1 content in the detergent-insoluble fraction (Figures 4B and 4D), robust binding to cellulose acetate membrane (Figure 4E, upper panel), and increased SDS-resistant higher molecular smear (Figure 4E, lower panel). Likewise, PINK1-positive aggregates were detected in N-recognin-deficient MEFs, but not in wild-type (WT) MEFs transiently transfected with WT PINK1 (Figure 4C and 4F). Although this aggregation was likely due to the accumulation of undegraded PINK1 species, we note that the $PINK1^{K137R}$ mutation, which also enhanced accumulation of PINK1 via failure to be ubiquitinated, did not promote aggregation; $PINK1^{K137R}$ did not differ from WT PINK1 in any of the four studied aggregation parameters (Figures 4B, 4D, and 4E). Thus, the greater stability of the 52-kDa PINK1 N-end-rule mutants likely reflected PINK1's propensity to aggregate rather than its susceptibility to degradation via an ostensible N-end rule mechanism.

Lastly, we examined the role of known E3 ligases that catalyze ubiquitination of mitochondrial proteins (Livnat-Levanon and Glickman, 2011). Consistent with our previous findings (Vives-Bauza et al., 2010), we found that silencing *Parkin* failed to attenuate PINK1

ubiquitination (Figure S4H). Likewise, silencing two main MOM-resident E3 ligases, namely, *MUL1* or *MARCH5* also failed to attenuate PINK1 ubiquitination (Figure S4I and S4J). These data suggest that PINK1 ubiquitination might be modulated by an E3 ligase other than those commonly involved in mitochondrial protein ubiquitination.

DISCUSSION

Here, we present evidence that PINK1 is degraded through a proteasome-dependent mechanism that relies on the preferential polyubiquitination of the mature 52-kDa form of the protein and that among its 20 internal lysine residues, one, K137, is critical for determining PINK1 ubiquitination. On the basis of our computational analyses, we believe that the preferential susceptibility of K137 to ubiquitination in 52-kDa PINK1 versus 63-kDa PINK1 is due to a conformational change in the mature protein that arises from the proteolytic removal of the first 103 aa of full-length PINK1, thereby exposing the site for ubiquitination. Indeed, K137 was predicted to reside in a region of structural flexibility in the protein's N-terminal region (between F104 and I233), with K137 exposed on the protein's surface (see Figure 3A). Dramatic conformational changes in transmembrane proteins following their proteolytic processing have been reported previously; prion protein, amyloid precursor protein, and cholera toxin typify this phenomenon (Hooper, 2005; Parkin et al., 2007; Ribi et al., 1988; Wernick et al., 2010).

Conformational changes, however, may not be the sole alteration that predisposes 52-kDa PINK1 to ubiquitination. Full-length PINK1, which we confirm here is an integral MOM protein (Sim et al., 2012; Zhou et al., 2008), is characterized by one main transmembrane domain of ~20 aa that includes a stretch of 14 consecutive hydrophobic amino acids, between A98 and I111. As proposed by the "mattress model" of lipid-protein interactions in membranes (Mouritsen and Bloom, 1984, 1993), it is energetically favorable for a membrane system to match a peptide's hydrophobic length to the bilayer's hydrophobic thickness. If this is the case with full-length versus mature PINK1, there will be a region of hydrophobic mismatch at the N-terminal portion of 52-kDa PINK1 due to the loss of the first 103 aa, including ~1/2 of the transmembrane domain, thereby rendering this hydrophobic sequence much shorter than the hydrophobic thickness of the MOM that it spans. Such phenomena have been shown to produce significant protein and membrane rearrangements (Dumas et al., 1999; Mouritsen and Bloom, 1993). Thus, we propose that the preferential ubiquitination of 52-kDa PINK1 results from the combination of PINK1 conformational changes and protein-membrane rearrangements that lead to a greater exposure of lysine residues and, in particular K137, to ubiquitination.

Although our data support the idea that mature PINK1 is degraded via ubiquitination, they do not support the view that the N-end rule is the primary means of PINK1 degradation as previously proposed (Yamano and Youle, 2013). Indeed, our analysis of PINK1 cellular accumulation showed that in our hands, the bulk of Ub-PINK1 is mitochondrially anchored and that the N-terminal phenylalanine (F104) of PINK1, which forms the N-degron motif, is located inside the MOM. Thus, the supposed PINK1 N-degron motif would be inaccessible to the cytosolically localized N-end rule ubiquitination machinery. Furthermore, we found that the extension of half-life in $F104^{M/A}$ mutants is due not to loss of the N-degron motif of

PINK1, but rather to an unexpected accumulation of aggregated (and poorly degradable) PINK1 species. Nonetheless, in healthy conditions, a small fraction of PINK1 is present in the cytosol (Beilina et al., 2005; Fedorowicz et al., 2014; Lin and Kang, 2008; Takatori et al., 2008; Weihofen et al., 2008). Thus, we cannot exclude that the cytosolic portion of PINK1, if it escapes ubiquitination while anchored in the mitochondria, might be degraded by the N-end rule pathway.

Remarkably, we also found that neither Parkin, Mach-5, or Mulan catalyze PINK1 ubiquitination, suggesting that PINK1 degradation does not rely on the most obvious cytosolic or mitochondrial E3 ubiquitin ligases in the context of the Parkin/PINK1 pathway. Previously, we and others have argued that PINK1 might reside at the mitochondrial contact sides (Silvestri et al., 2005; Zhou et al., 2008). More recently, it has been reported that PINK1 may be localized at the mitochondria-associated membranes (Gelmetti et al., 2017). Thus, PINK1 may be an ideal candidate for trans-ubiquitination by E3 ubiquitin ligases embedded in organelles other than mitochondria.

Unlike most substrates destined for proteasomal degradation, we found that PINK1 polyubiquitin chains are not made solely of K48 linkages, but of K29 and, to a lesser extent, K63 linkages as well. The occurrence of K29-dependent heterotypic ubiquitin chains suggests that PINK1 ubiquitination is initiated by short K29 chains that serve as a scaffold for subsequent assembly of longer chains made primarily of K48 linkages (Kristariyanto et al., 2015; Michel et al., 2015). Because the length of the K48-linked chain profoundly influences the targeting of the substrate to the proteasome (Pickart and Fushman, 2004), the K29 linkages are likely necessary but not sufficient to promote PINK1 degradation.

Taken together, our data support the following model of PINK1 homeostasis. Upon translation of PINK1, the N-terminal part of the full-length 63-kDa protein is imported into mitochondria, where the first 103 amino acids are removed by the combination of MPP and PARL proteases, producing 52-kDa PINK1. This shorter form of PINK1 adopts a distinct conformation and engages in interactions with bilayer membranes in a manner distinct from that of the 63-kDa form. In turn, this modified conformation promotes exposure of K137 in the region linking the transmembrane and kinase domains that is critical for modification of 52-kDa PINK1 by ubiquitin. Thus, the molecular pathway outlined here allows PINK1 ubiquitination to be tightly regulated in a timely and spatially restricted manner and ensures that PINK1 serves its function as a mitochondrial quality control factor. Our data are not consistent with PINK1 ubiquitination being primarily, if at all, catalyzed by either the N-end rule or mitochondrial associated E3 ligases (Figures S4H, S4I, and S4J), and thus the exact details that decipher how Ub-PINK1 is generated and accesses the proteasome are currently under investigation.

EXPERIMENTAL PROCEDURES

Cell Culture, Transfection, and Plasmids

MEF Ubr1$^{-/-}$ Ubr2$^{-/-}$ Ubr4^{siRNA} (where Ubr4 was knocked down by siRNA in double Ubr1- and Ubr2-deficient cells) and Parl$^{-/-}$ cells were generous gifts from Yong Tae Kwon (University of Pittsburgh) and Bart de Strooper (KU Leuven, Belgium), respectively.

Transient transfections were performed as previously described (Becker et al., 2012; Vives-Bauza et al., 2010). Epitope-tagged PINK1 and PINK1 mutants or deletion constructs were generated by PCR-based DNA mutagenesis.

Subcellular Fractionation, Protease K Protection Assay, and Alkaline Extraction

Crude mitochondria from cultured cells were fractioned as described previously (Area-Gomez, 2014; Bozidis et al., 2007; Guardia-Laguarta et al., 2014). The protease K protection assay and alkaline extraction were performed as described (Zhou et al., 2008).

Immunoblotting, Immunoprecipitation, and In Vivo Ubiquitination

Immunoblotting and immunoprecipitation assays were carried out as previously described (Vives-Bauza et al., 2010; Zhou et al., 2008). For in vivo ubiquitination assay, cell lysates were boiled in 1% SDS-containing buffer prior to being immunoprecipitated with a polyclonal anti-PINK1 antibody. Then, ubiquitinated species were revealed by immunoblotting analysis using an antibody against HA or ubiquitin.

Filter Trap Assay for Protein Aggregates

As described previously (Scherzinger et al., 1999; Wanker et al., 1999), a total of 200 μg of cell lysate was applied to 0.22 μM cellulose acetate membrane (NitroBind) in a dot blotting apparatus, followed by immunoblotting with anti-PINK1.

Protein Half-Life Assay

PINK1 half-life assay was performed in HeLa or MEF cells that transiently or stably express PINK1 using cycloheximide (100 μg/mL) similarly as described (Liu et al., 2007).

Immunofluorescence and Imaging

All procedures were previously described (Guardia-Laguarta et al., 2014).

Structural Modeling of the 52-kDa PINK1

The i-TASSER program (Roy et al., 2010; Zhang, 2008) was used to predict the three-dimensional structure of the 52-kDa PINK1. Top predicted structural models were selected based on the C-score and stereochemical quality, as indicated by PROCHECK (Laskowski et al., 1993). For homology modeling, we used BlastP to identify suitable structural templates in the Protein Data Bank, and the program Modeler (Sali and Blundell, 1993) was employed to predict the kinase domain of PINK1.

Mass Spectrometry Analysis

PINK1-purified protein complexes were resolved using SDS-polyacrylamide gel electrophoresis, and protein bands were excised, digested with trypsin, and purified using Poros 50 R2 (Applied Biosystems) reversed-phased beads. Then, purified peptide mixtures were subjected to nano LC-MS/MS analysis as described (Beverly et al., 2012).

Statistical Analysis

Data are presented as mean ± SEM from at least three independent experiments. Samples were compared by one- or two-way ANOVA followed by a Student's-Newman-Keuls test. The Null hypothesis was rejected at the 0.05 level. All analyses were performed with Sigmaplot for Windows version 12.0 (Systech Software).

Supplementary Material

Refer to Web version on PubMed Central for supplementary material.

Acknowledgments

We thank Timothy Bromage for help on mass spectra figure preparation and Zhezheng Li and Kevin Velasco for technical support on cell culture and plasmid constructions. We thank Eric A. Schon for insightful comments and editing the manuscript and Yihong Ye, Estela Area-Gomez, Vernice Jackson-Lewis, Andrew Koff, Pengbo Zhou, and David Volsky for helpful discussions and suggestions. X.J. was supported by NIH grants R01CA166413 and R01GM113013, Mr. William H. and Mrs. Alice Goodwin, and the Commonwealth Foundation for Cancer Research of the MSKCC Experimental Therapeutics Center. X.J. was also supported by NCI Cancer Center support grant P30 CA008748 to MSKCC. C.G-L. was supported by the American Parkinson Disease Association grant CU14-1059. S.P. was supported by NIH grants R01 NS072428-04 and R21 NS099862-A1 and Department of Defense grant W81XWH-13-1-0416.

References

Area-Gomez E. Assessing the function of mitochondria-associated ER membranes. Methods Enzymol. 2014; 547:181–197. [PubMed: 25416359]

Becker D, Richter J, Tocilescu MA, Przedborski S, Voos W. Pink1 kinase and its membrane potential (Deltaψ)-dependent cleavage product both localize to outer mitochondrial membrane by unique targeting mode. J Biol Chem. 2012; 287:22969–22987. [PubMed: 22547060]

Beilina A, Van Der Brug M, Ahmad R, Kesavapany S, Miller DW, Petsko GA, Cookson MR. Mutations in PTEN-induced putative kinase 1 associated with recessive parkinsonism have differential effects on protein stability. Proc Natl Acad Sci USA. 2005; 102:5703–5708. [PubMed: 15824318]

Beverly LJ, Lockwood WW, Shah PP, Erdjument-Bromage H, Varmus H. Ubiquitination, localization, and stability of an anti-apoptotic BCL2-like protein, BCL2L10/BCLb, are regulated by Ubiquilin1. Proc Natl Acad Sci USA. 2012; 109:E119–E126. [PubMed: 22233804]

Blackinton JG, Anvret A, Beilina A, Olson L, Cookson MR, Galter D. Expression of PINK1 mRNA in human and rodent brain and in Parkinson's disease. Brain Res. 2007; 1184:10–16. [PubMed: 17950257]

Bozidis, P., Williamson, CD., Colberg-Poley, AM. Current Protocols in Cell Biology. John Wiley & Sons; 2007. Isolation of endoplasmic reticulum, mitochondria, and mitochondria-associated membrane fractions from transfected cells and from human cytomegalovirus-infected primary fibroblasts; p. 3.27.1-3.27.23.

Dauer W, Przedborski S. Parkinson's disease: mechanisms and models. Neuron. 2003; 39:889–909. [PubMed: 12971891]

Deas E, Plun-Favreau H, Gandhi S, Desmond H, Kjaer S, Loh SH, Renton AE, Harvey RJ, Whitworth AJ, Martins LM, et al. PINK1 cleavage at position A103 by the mitochondrial protease PARL. Hum Mol Genet. 2011; 20:867–879. [PubMed: 21138942]

Dumas F, Lebrun MC, Tocanne JF. Is the protein/lipid hydrophobic matching principle relevant to membrane organization and functions? FEBS Lett. 1999; 458:271–277. [PubMed: 10570923]

Fedorowicz MA, de Vries-Schneider RL, Rüb C, Becker D, Huang Y, Zhou C, Alessi Wolken DM, Voos W, Liu Y, Przedborski S. Cytosolic cleaved PINK1 represses Parkin translocation to mitochondria and mitophagy. EMBO Rep. 2014; 15:86–93. [PubMed: 24357652]

Gelmetti V, De Rosa P, Torosantucci L, Marini ES, Romagnoli A, Di Rienzo M, Arena G, Vignone D, Fimia GM, Valente EM. PINK1 and BECN1 relocalize at mitochondria-associated membranes during mitophagy and promote ER-mitochondria tethering and autophagosome formation. Autophagy. 2017; 13:654–669. [PubMed: 28368777]

Greene AW, Grenier K, Aguileta MA, Muise S, Farazifard R, Haque ME, McBride HM, Park DS, Fon EA. Mitochondrial processing peptidase regulates PINK1 processing, import and Parkin recruitment. EMBO Rep. 2012; 13:378–385. [PubMed: 22354088]

Guardia-Laguarta C, Area-Gomez E, Rüb C, Liu Y, Magrané J, Becker D, Voos W, Schon EA, Przedborski S. α-Synuclein is localized to mitochondria-associated ER membranes. J Neurosci. 2014; 34:249–259. [PubMed: 24381286]

Hooper NM. Roles of proteolysis and lipid rafts in the processing of the amyloid precursor protein and prion protein. Biochem Soc Trans. 2005; 33:335–338. [PubMed: 15787600]

Jin SM, Lazarou M, Wang C, Kane LA, Narendra DP, Youle RJ. Mitochondrial membrane potential regulates PINK1 import and proteolytic destabilization by PARL. J Cell Biol. 2010; 191:933–942. [PubMed: 21115803]

Kravtsova-Ivantsiv Y, Sommer T, Ciechanover A. The lysine48-based polyubiquitin chain proteasomal signal: not a single child anymore. Angew Chem Int Ed Engl. 2013; 52:192–198. [PubMed: 23124625]

Kristariyanto YA, Abdul Rehman SA, Campbell DG, Morrice NA, Johnson C, Toth R, Kulathu Y. K29-selective ubiquitin binding domain reveals structural basis of specificity and heterotypic nature of k29 polyubiquitin. Mol Cell. 2015; 58:83–94. [PubMed: 25752573]

Laskowski RA, MacArthur MW, Moss DS, Thornton JM. PROCHECK: a program to check the stereochemical quality of protein structures. J Appl Cryst. 1993; 26:283–291.

Lin W, Kang UJ. Characterization of PINK1 processing, stability, and subcellular localization. J Neurochem. 2008; 106:464–474. [PubMed: 18397367]

Liu Y, Yeh N, Zhu XH, Leversha M, Cordon-Cardo C, Ghossein R, Singh B, Holland E, Koff A. Somatic cell type specific gene transfer reveals a tumor-promoting function for p21(Waf1/Cip1). EMBO J. 2007; 26:4683–4693. [PubMed: 17948060]

Livnat-Levanon N, Glickman MH. Ubiquitin-proteasome system and mitochondria - reciprocity. Biochim Biophys Acta. 2011; 1809:80–87. [PubMed: 20674813]

Michel MA, Elliott PR, Swatek KN, Simicek M, Pruneda JN, Wagstaff JL, Freund SM, Komander D. Assembly and specific recognition of k29- and k33-linked polyubiquitin. Mol Cell. 2015; 58:95–109. [PubMed: 25752577]

Mouritsen OG, Bloom M. Mattress model of lipid-protein interactions in membranes. Biophys J. 1984; 46:141–153. [PubMed: 6478029]

Mouritsen OG, Bloom M. Models of lipid-protein interactions in membranes. Annu Rev Biophys Biomol Struct. 1993; 22:145–171. [PubMed: 8347987]

Narendra DP, Jin SM, Tanaka A, Suen DF, Gautier CA, Shen J, Cookson MR, Youle RJ. PINK1 is selectively stabilized on impaired mitochondria to activate Parkin. PLoS Biol. 2010; 8:e1000298. [PubMed: 20126261]

Parkin ET, Watt NT, Hussain I, Eckman EA, Eckman CB, Manson JC, Baybutt HN, Turner AJ, Hooper NM. Cellular prion protein regulates beta-secretase cleavage of the Alzheimer's amyloid precursor protein. Proc Natl Acad Sci USA. 2007; 104:11062–11067. [PubMed: 17573534]

Pickart CM, Fushman D. Polyubiquitin chains: polymeric protein signals. Curr Opin Chem Biol. 2004; 8:610–616. [PubMed: 15556404]

Ribi HO, Ludwig DS, Mercer KL, Schoolnik GK, Kornberg RD. Three-dimensional structure of cholera toxin penetrating a lipid membrane. Science. 1988; 239:1272–1276. [PubMed: 3344432]

Roy A, Kucukural A, Zhang Y. I-TASSER: a unified platform for automated protein structure and function prediction. Nat Protoc. 2010; 5:725–738. [PubMed: 20360767]

Sali A, Blundell TL. Comparative protein modelling by satisfaction of spatial restraints. J Mol Biol. 1993; 234:779–815. [PubMed: 8254673]

Scherzinger E, Sittler A, Schweiger K, Heiser V, Lurz R, Hasenbank R, Bates GP, Lehrach H, Wanker EE. Self-assembly of polyglutamine-containing huntingtin fragments into amyloid-like fibrils:

implications for Huntington's disease pathology. Proc Natl Acad Sci USA. 1999; 96:4604–4609. [PubMed: 10200309]

Shiba K, Arai T, Sato S, Kubo S, Ohba Y, Mizuno Y, Hattori N. Parkin stabilizes PINK1 through direct interaction. Biochem Biophys Res Commun. 2009; 383:331–335. [PubMed: 19358826]

Silvestri L, Caputo V, Bellacchio E, Atorino L, Dallapiccola B, Valente EM, Casari G. Mitochondrial import and enzymatic activity of PINK1 mutants associated to recessive parkinsonism. Hum Mol Genet. 2005; 14:3477–3492. [PubMed: 16207731]

Sim CH, Gabriel K, Mills RD, Culvenor JG, Cheng HC. Analysis of the regulatory and catalytic domains of PTEN-induced kinase-1 (PINK1). Hum Mutat. 2012; 33:1408–1422. [PubMed: 22644621]

Sriram SM, Kwon YT. The molecular principles of N-end rule recognition. Nat Struct Mol Biol. 2010; 17:1164–1165. [PubMed: 20924402]

Takatori S, Ito G, Iwatsubo T. Cytoplasmic localization and proteasomal degradation of N-terminally cleaved form of PINK1. Neurosci Lett. 2008; 430:13–17. [PubMed: 18031932]

Tanaka A, Cleland MM, Xu S, Narendra DP, Suen DF, Karbowski M, Youle RJ. Proteasome and p97 mediate mitophagy and degradation of mitofusins induced by Parkin. J Cell Biol. 2010; 191:1367–1380. [PubMed: 21173115]

Taymans JM, Van den Haute C, Baekelandt V. Distribution of PINK1 and LRRK2 in rat and mouse brain. J Neurochem. 2006; 98:951–961. [PubMed: 16771836]

Unoki M, Nakamura Y. Growth-suppressive effects of BPOZ and EGR2, two genes involved in the PTEN signaling pathway. Oncogene. 2001; 20:4457–4465. [PubMed: 11494141]

Valente EM, Abou-Sleiman PM, Caputo V, Muqit MM, Harvey K, Gispert S, Ali Z, Del Turco D, Bentivoglio AR, Healy DG, et al. Hereditary early-onset Parkinson's disease caused by mutations in PINK1. Science. 2004; 304:1158–1160. [PubMed: 15087508]

Varshavsky A. The N-end rule pathway and regulation by proteolysis. Protein Sci. 2011; 20:1298–1345. [PubMed: 21633985]

Vives-Bauza C, Zhou C, Huang Y, Cui M, de Vries RL, Kim J, May J, Tocilescu MA, Liu W, Ko HS, et al. PINK1-dependent recruitment of Parkin to mitochondria in mitophagy. Proc Natl Acad Sci USA. 2010; 107:378–383. [PubMed: 19966284]

Wanker EE, Scherzinger E, Heiser V, Sittler A, Eickhoff H, Lehrach H. Membrane filter assay for detection of amyloid-like polyglutamine-containing protein aggregates. Methods Enzymol. 1999; 309:375–386. [PubMed: 10507036]

Weihofen A, Ostaszewski B, Minami Y, Selkoe DJ. Pink1 Parkinson mutations, the Cdc37/Hsp90 chaperones and Parkin all influence the maturation or subcellular distribution of Pink1. Hum Mol Genet. 2008; 17:602–616. [PubMed: 18003639]

Wernick NL, De Luca H, Kam WR, Lencer WI. N-terminal extension of the cholera toxin A1-chain causes rapid degradation after retro-translocation from endoplasmic reticulum to cytosol. J Biol Chem. 2010; 285:6145–6152. [PubMed: 20056601]

Whitworth AJ, Lee JR, Ho VM, Flick R, Chowdhury R, McQuibban GA. Rhomboid-7 and HtrA2/Omi act in a common pathway with the Parkinson's disease factors Pink1 and Parkin. Dis Model Mech. 2008; 1:168–174. [PubMed: 19048081]

Yamano K, Youle RJ. PINK1 is degraded through the N-end rule pathway. Autophagy. 2013; 9:1758–1769. [PubMed: 24121706]

Zhang Y. I-TASSER server for protein 3D structure prediction. BMC Bioinformatics. 2008; 9:40. [PubMed: 18215316]

Zhou C, Huang Y, Shao Y, May J, Prou D, Perier C, Dauer W, Schon EA, Przedborski S. The kinase domain of mitochondrial PINK1 faces the cytoplasm. Proc Natl Acad Sci USA. 2008; 105:12022–12027. [PubMed: 18687899]

Highlights

- Mature PINK1 is regulated by ubiquitination and degradation by the proteasome
- Ubiquitinated PINK1 is anchored to mitochondria
- The 52-kDa mature PINK1 is the target of polyubiquitination
- K137 is the main site for ubiquitination of mitochondrial PINK1

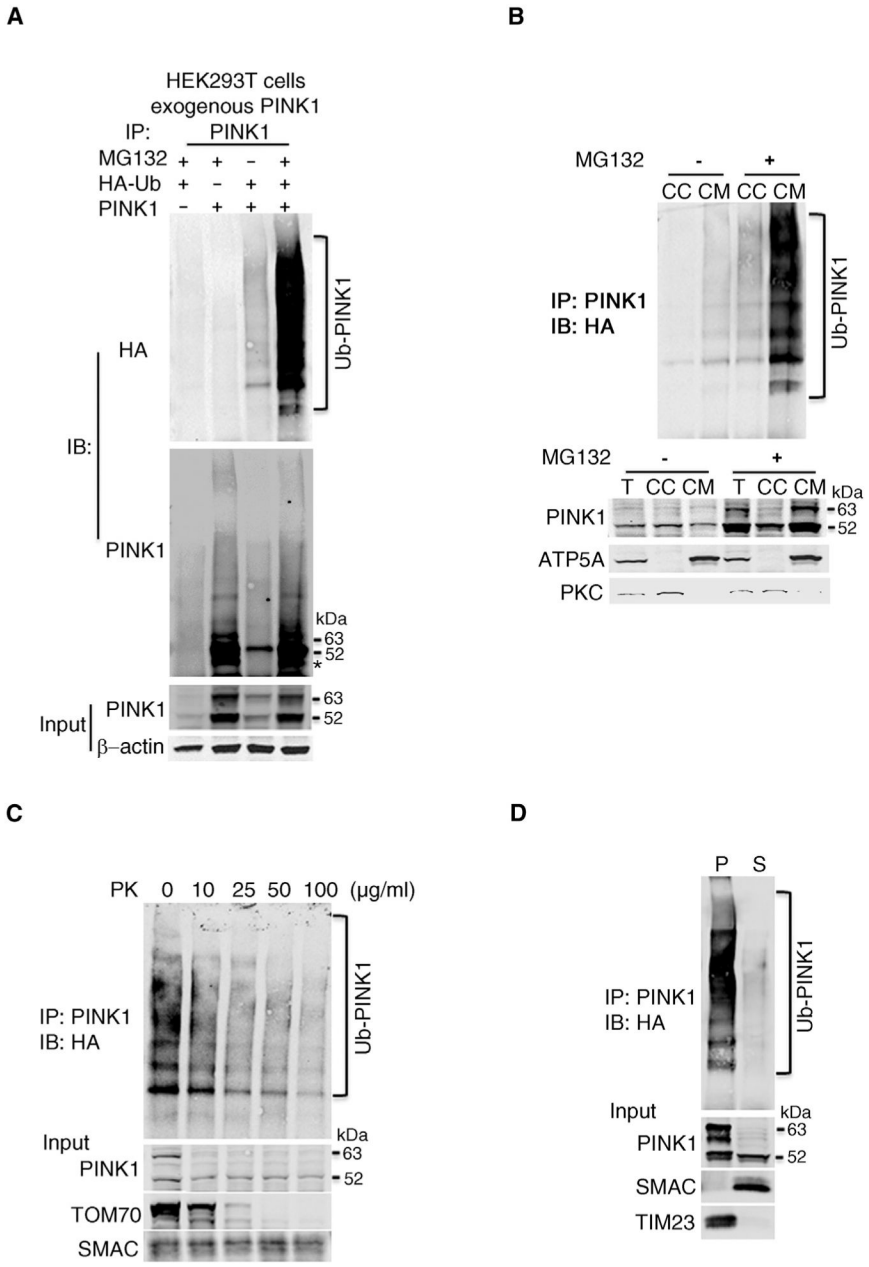

Figure 1. Ubiquitinated PINK1 Is Associated with Mitochondria and Faces the Cytosol

(A) In vivo ubiquitination assay in HEK293T cells co-transfected with HA-Ub and WT PINK1 constructs were incubated for 6 hr with 10 μM MG132. IB, immunoblotting. IBs were re-probed with anti-PINK1 antibody. Input was 10% of the extracts. *Immunoglobulin G (IgG) heavy chain.

(B) Subcellular fractionation of Ub-PINK1. T, total cell extracts; CC, crude cytosol; CM, crude mitochondrial fractions from HA-Ub and PINK1 co-transfected HEK293T cells exposed to MG132. Anti-PINK1 antibody for IP raised against aa 175–250 (denoted “PINK1”). Input is 10% of T, CC, or CM. ATPase alpha (ATP5A) and protein kinase C (PKC) are mitochondrial and cytosolic markers, respectively.

(C) PK effects on Ub-PINK1 from crude mitochondrial fractions. TOM70 and SMAC are MOM and IMS protein markers, respectively.
(D) Effect of alkaline extraction (0.1 M Na_2CO_3, pH 11) on Ub-PINK1 from crude mitochondrial fractions. p, particulate fraction; S, supernatant. TIM23 and SMAC are mitochondrial integral membrane and soluble protein markers, respectively.

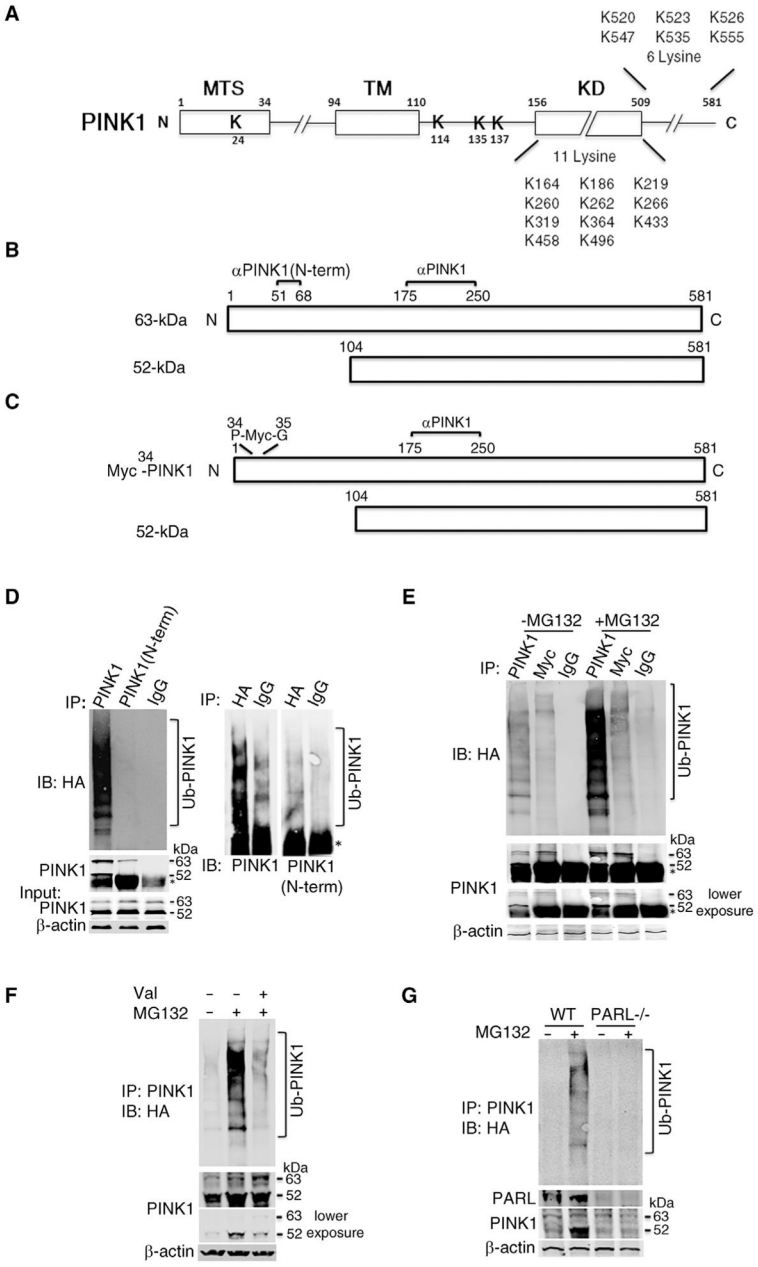

Figure 2. The 52-kDa Cleaved PINK1 Is the Predominant Ubiquitinated Species

(A) Schematic of human PINK1 protein functional domains and location of its 21 lysine residues (K). MTS, mitochondrial targeting sequence; TM, transmembrane domain; KD, kinase domain.

(B) Diagram of PINK1 regions recognized by anti-PINK1 N-term and BC100-494 (denoted as PINK1 antibody on the rest of the figures) antibodies.

(C) Schematic of the Myc^{34}-PINK1 construct.

(D) Left: Ub-PINK1 IP of HEK293T cells with either anti-PINK1 antibody PINK1 or N-term and IB with anti-HA antibody. Right: reversed IP using anti-HA antibody or pre-

immune IgG (control) and then IB with either the PINK1 or N-term antibody. *52-kDa PINK1 migrates slightly above the heavy chain of IgG.

(E) Similar experiment as in (D). Left: cells co-transfected with Myc^{34}-PINK1 and HA-Ub using anti-PINK1 or anti-Myc antibody for IP and anti-HA antibody for IB.

(F) PINK1 IP of HEK293T cells overexpressing PINK1 and HA-Ub exposed to 1 μm valinomycin (Val) for 12 hr, and then to 10 μm MG132 for 6 hr. IB with Ub-PINK1 from total extracts.

(G) PINK1 IP of total extracts from WT or PALS-deficient ($PARL^{-/-}$) MEF overexpressing PINK1 and HA-Ub. IB with anti Ub-PINK1.

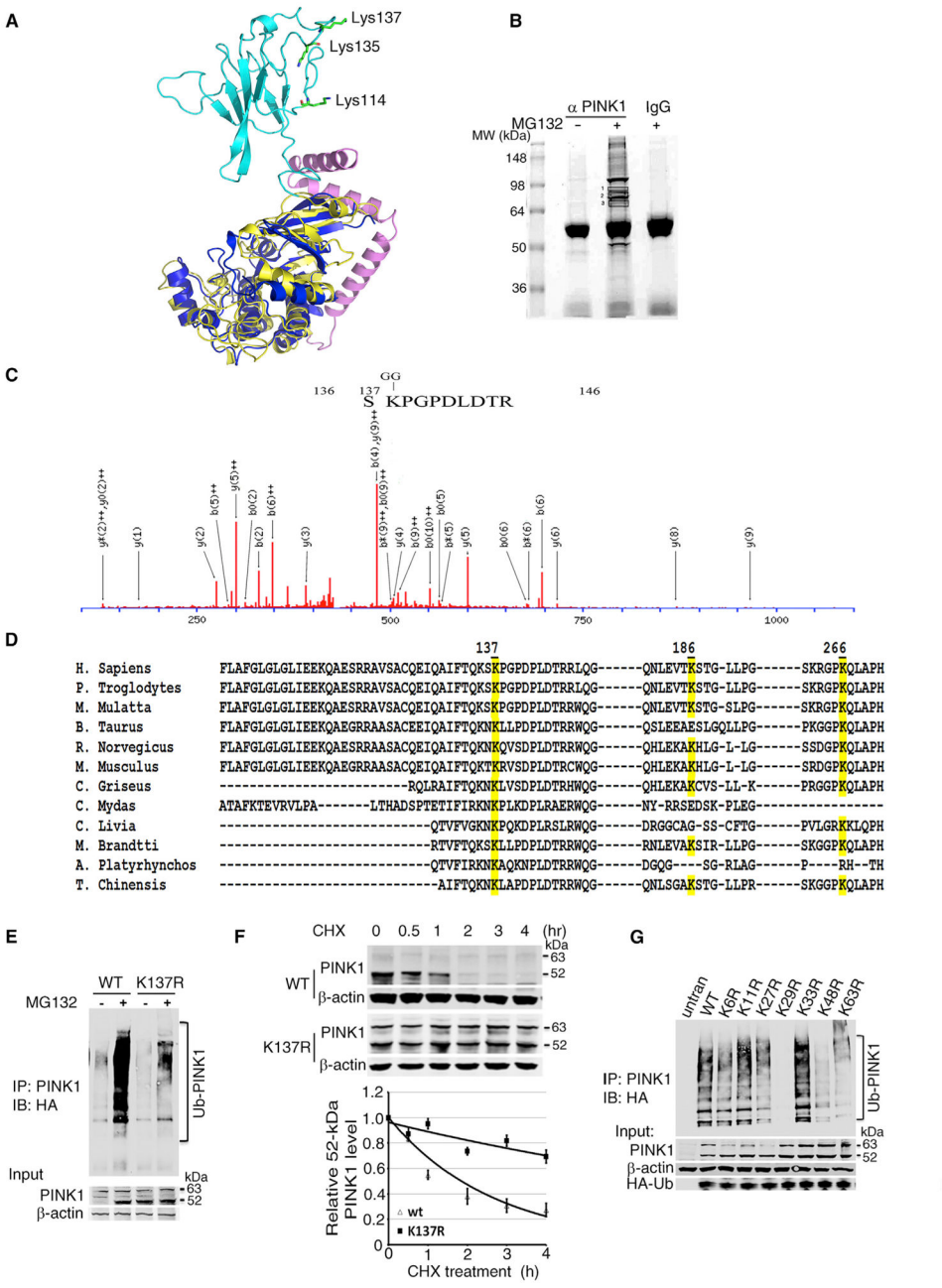

Figure 3. Lys137 Is the Major Ubiquitination Site of PINK1

(A) Predicted 3D model of the 52-kDa PINK1. The linker region, kinase domain, and C terminus are shown in cyan, yellow, and violet, respectively. An experimentally determined kinase domain (PDB: 3DXN) is aligned to the kinase domain of PINK1 and colored in blue (root-mean-square deviation [RMSD] 2.3 Å over 145 Cα pairs). Lys114, Lys135, and Lys137 of PINK1 are shown as sticks.

(B) PINK1 ubiquitination sites by mass spectrometry. Bands labeled 1–3 were excised from the gel and analyzed by mass spectrometry to identify the -Gly-Gly signature. Ub-PINK1 was enriched by IP with the anti-PINK1 antibody using lysates from PINK1 and HA-Ub co-

transfected HEK293T cells exposed to MG132. Eluted proteins were stained with Coomassie blue. Pre-immune IgG was used as control.

(C) Lys137, Lys186, and Lys266 (see Figure S3A) are the sites identified with the -Gly-Gly signature.

(D) Sequence alignment of ubiquitin-modified lysine residues (Lys137, Lys186, and Lys266) and the linker region connecting the TM and KD domain of PINK1 orthologs.

(E) Ub-PINK1 IB from HA-Ub and PINK1^{K137R} co-transfected HEK293T cells.

(F) Half-life of WT PINK1 or mutant PINK1^{K137R} by IB using anti-PINK1 antibody. HeLa cells were incubated with 10 μM MG132 for 2 hr and then, after wash-out, with 100 μg/mL of cycloheximide (CHX). Cells were harvested at the indicated time points. Upper: representative IB. Bottom: IB quantification. Data are presented as mean ± SEM from at least three independent experiments.

(G) Same as Figure 1A, except that different HA-Ub mutant constructs were used for co-transfection.

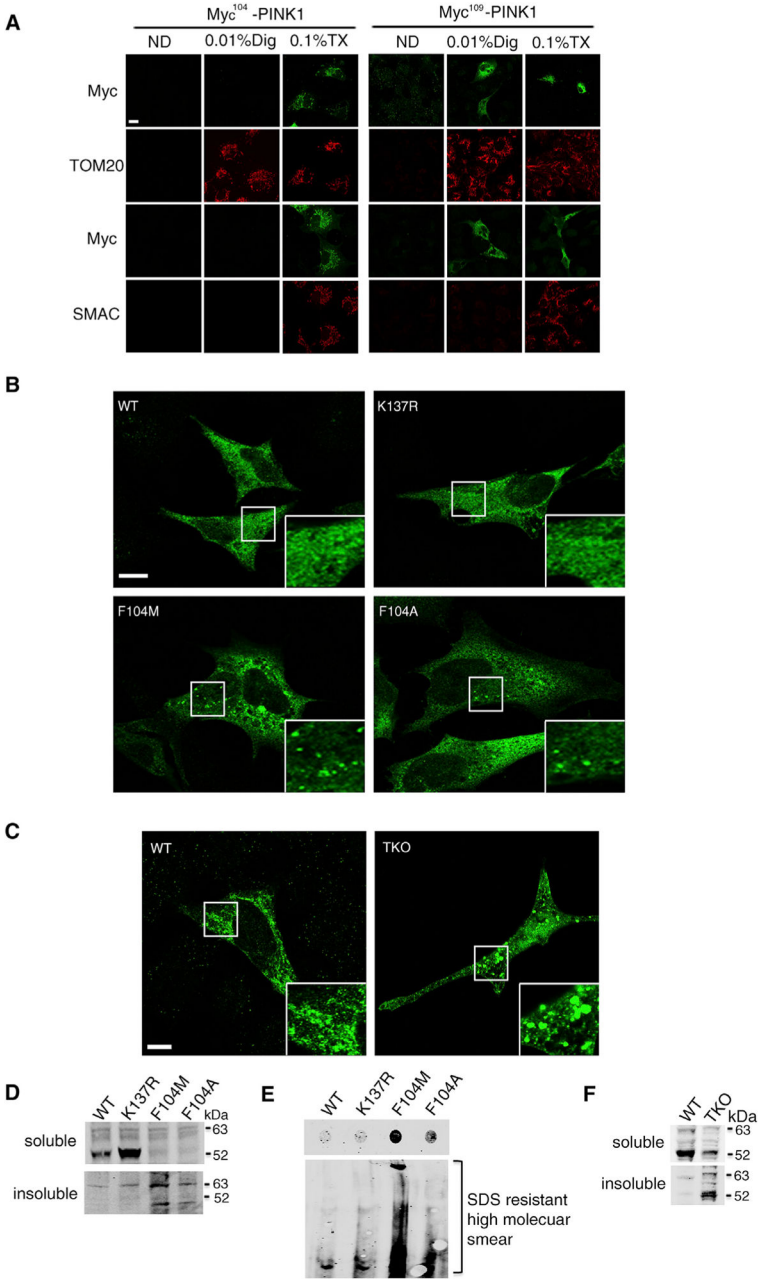

Figure 4. Ubiquitination of 52-kDa PINK1 May Not Be Related to the N-End Rule Process

(A) HeLa cells transfected with either Myc^{104}-PINK1 or Myc^{109}-PINK1 construct. Permeabilization was performed by 0.01% digitonin (Dig) or 0.1% Triton X-100 (TX) before immunofluorescence. ND, non-detergent-treated control. Scale bar, 10 μm.

(B) PINK1 immunofluorescence of WT or mutant PINK1 transiently transfected HeLa cells. Scale bar, 10 μm.

(C) PINK1 immunofluorescence of transiently transfected WT or ubr1$^{-/-}$ubr2$^{-/-}$ubr4^{siRNA} triple knockout (TKO) mutant MEF cells. Scale bar, 10 μm.

(D) PINK1 transfected HeLa Cells were extracted using 1% NP40 lysis buffer, and insoluble pellets were resolubilized in the Laemmli buffer.

(E) Upper: filter trap assay of cell lysates from WT and mutant PINK1 transfected HEK293T. Lower: same cell lysates as upper panel showing detergent-resistant high molecular smear.

(F) Same as in (D), except that WT or ubr1$^{-/-}$ubr2$^{-/-}$ubr4^{siRNA} (TKO) MEF cells were transfected with WT PINK1 construct.